Scientia Iranica, Vol. 15, No. 3, pp 295–307

SCIENTIA IRANICA

Performance Evaluation of Masonry Buildings Using a Probabilistic Approach

A. Bakhshi* **and K. Karimi**[1]

In many countries, there are traditional houses made of stone, adobe and brick, which perform relatively weakly in earthquakes. To mitigate casualties in future earthquakes, it is necessary to evaluate the current status of these buildings and propose effective methods to retrofit them. One method of evaluating the performance of buildings in earthquakes is through the use of fragility curves. These diagrams show the probability of exceeding a specific state of damage versus seismic intensity parameters, such as PGA, MMI, Ia, CAV etc. Fragility curves will provide an important basis for analytical methods, based on probabilistic approaches. Much work has been done on bridges, concrete and steel structures, while limited studies have been conducted on masonry buildings. Considering the prevalence of these buildings and the high seismic activity in some regions where they are built, fragility curves for different types of masonry buildings are developed in this research. The results obtained show the probable damage to those types of masonry building chosen in this research for different earthquake intensities and restates that, by providing horizontal and vertical ties and retrofitting these buildings, by the methods proposed in some seismic code provisions (such as FEMA 356 and 357), their behavior in earthquakes are apparently effected and structural damage reduced. Furthermore, results indicate that soil type does not significantly influence the seismic behavior of masonry buildings.

INTRODUCTION

Each year earthquakes occur in several countries, killing many people and causing extreme loss. It is obvious that unreinforced masonry buildings are among the most vulnerable structures in earthquakes.

These buildings are traditionally made of low-strength materials, such as brick or adobe, without any structural system to resist earthquakes. Therefore, evaluating the seismic performance of these buildings and proposing some effective methods to rehabilitate them against earthquakes is an essential step toward hazard mitigation and risk assessment.

Developing fragility curves for a specific type of building is a probabilistic method to estimate the probability that the building will exceed a specific state of damage for a definite value of the seismic intensity parameter. This parameter can be taken as PGA, MMI, I_a, CAV and so on. Usually, PGA (Peak Ground Acceleration) is used as the seismic intensity parameter in developing fragility curves, but, in this paper, CAV (Cumulative Absolute Velocity) has been chosen for this purpose, since it is found to be well associated with structural damage [1].

Fragility Curves are categorized into two types: Empirical and Analytical. Empirical fragility curves are developed using real damage data, obtained from previously occurred earthquakes, while analytical fragility curves are constructed, based on nonlinear dynamic analysis. Much work has been done on developing fragility curves for some types of structure, such as bridges [2,3], reinforced concrete structures [4-6] and tall buildings [7]. However, not sufficient effort has been made toward developing fragility curves for masonry buildings, especially the unreinforced ones, which are very common in several countries and which are much more vulnerable to earthquake than many other types of building.

In this paper, analytical fragility curves are developed for masonry buildings, before and after using seismic provisions and retrofitting. Uncertainty is considered in some structural parameters, including the compressive and tensile strength of the brick laying unit, the compressive strength of the concrete and

*. *Corresponding Author, Department of Civil Engineering, Sharif University of Technology, P.O. Box 11155-9313, Tehran, Iran. E-mail: bakhshi@sharif.edu*

1. *Department of Civil Engineering, Sharif University of Technology, Tehran, Iran.*

the tensile strength of the reinforcing bars. For developing each fragility curve, 15 different models are made, based on the values for uncertain structural parameters, which are resulted from the Monte Carlo Simulation method [8]. These models are analyzed under various earthquake records using the IDARC 4.0 nonlinear analysis program [9]. Twelve earthquake records are used in this study; half of which are recorded on rock and the rest of which on soil sites. Hence, separate fragility curves are obtained for different site conditions. Also, two types of masonry building are considered, based on the number of stories that is, one and three-stories. Seismic damage cost and the effect of different parameters, such as number of stories, site condition, horizontal and vertical ties and reinforcing bars, on the seismic performance of masonry buildings is further investigated, using the obtained fragility curves. Finally, the results obtained in this research are verified through comparison with some other works done in this area.

SELECTION OF EARTHQUAKE RECORDS

As noted earlier, 12 Earthquake records are used in this paper. They are selected, such that each site provides sufficient records for both rock and soil sites. The near fault effect is also considered in choosing some of these records. The records used in this research are shown in Table 1, with their corresponding seismic parameters, including CAV (Cumulative Absolute Velocity), a_{rms} (root mean square of accelerations), I_a (Arias intensity), I_c (characteristic intensity), $C.F.$ (Central Frequency), $S.F.$ (Shape Factor), $M.P.A.$ (Median Peak Acceleration) and T_{Dominant} (dominant period). These parameters are defined and discussed in another paper by the authors [1].

CAV, which is used frequently in this paper as the seismic intensity parameter in developing fragility curves, is well recognized as follows:

$$CAV = \int_0^T |a(t)dt|, \tag{1}$$

where $a(t)$ is the ground acceleration time history and T is the duration of the earthquake. Since most of the design engineers are more familiar with PGA than CAV, the relation between these two parameters for the selected records is shown in Figure 1.

DAMAGE STATES AND DAMAGE INDICES

When buildings are subjected to earthquakes, various states of damage occur. In this paper, five damage states are considered:

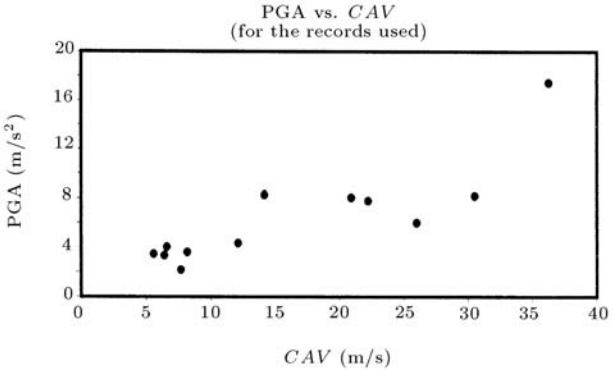

Figure 1. Correlation between PGA and CAV for the selected earthquake records.

1. Nonstructural damage,
2. Slight structural damage,
3. Moderate structural damage,
4. Severe structural damage,
5. Collapse.

These damage states are defined, using the damage index proposed by Park and Ang [10,11].

The Park and Ang damage index for a structural element is defined as follows [11]:

$$DI_{PA} = \frac{\phi_m - \phi_y}{\phi_u - \phi_y} + \frac{\beta_e}{M_y \phi_u} \int dE, \tag{2}$$

where:

ϕ_m = Maximum curvature caused by an earthquake,
ϕ_y = Yield curvature,
ϕ_u = Ultimate deformation under monotonic loading,
$\int dE$ = Cumulative dissipated energy,
M_y = Yield moment,
β_e = Coefficient related to structural types.

The building damage index will, further, be obtained on the basis of its individual element damage indices. The range and best-estimate values of the building damage index, DT, corresponding to various states of damage, are shown in Table 2.

FRAGILITY CURVES AND DAMAGE PROBABILITY MATRIX

The probability PF_{ij}, that the damage exceeds the ith damage state, given the occurrence of an earthquake with CAV equal to v_j, can be determined as follows:

$$PF_{ij} = \text{prob}(DT \geq DT_i | CAV = v_j)$$
$$= F_{DT}(DT_i | CAV = v_j), \tag{3}$$

Table 1. Earthquake records on rock and soil sites, used in this paper.

Records on Rock						
Earthquake	**Kocaeli**	**Tabas**	**Loma Prieta**	**Kobe**	**Northridge**	**Friuli**
Date	**17/8/1999**	**16/9/1978**	**18/10/1989**	**16/1/1995**	**17/1/1994**	**6/5/1976**
Station	**Izmit**	**Tabas**	**Gilroy#1**	**KJMA**	**Tarzana**	**Tolmezzo**
Component	**090**	**LN**	**000**	**000**	**090**	**000**
PGA **(m/s/s)**	2.154	8.199	4.031	8.057	17.456	3.443
PGV **(m/s)**	0.298	0.978	0.316	0.813	1.136	0.220
PGD **(m)**	0.171	0.369	0.064	0.177	0.332	0.041
Soil Type (Geomatrix)	Rock	Deep (narrow) soil	Rock	Shallow (stiff) soil	Shallow (stiff) soil	Shallow (stiff) soil
$T_{(\text{total})}$ **(s)**	30.000	32.860	39.950	48.000	40.000	36.345
$T_{(\text{Page-Bolt})}$ **(s)**	24.005	27.220	13.250	21.400	27.320	7.415
T_{Trifunac} **(s)**	13.242	16.487	6.530	8.351	10.538	4.245
CAV **(m/s)**	7.678	30.529	6.596	20.913	36.294	5.571
a_{rms} **(m/s/s)**	0.460	1.627	0.705	1.565	2.280	0.811
I_a **(m/s)**	0.813	11.543	1.055	8.391	22.748	0.780
I_c **(m$^{1.5}$/S$^{2.5}$)**	1.528	10.832	2.156	9.055	17.999	1.988
C.F. **(Hz)**	3.823	5.207	6.969	2.343	5.623	4.130
S.F.	0.604	0.599	0.612	0.507	0.643	0.547
M.P.A. **(m/s/s)**	1.521	5.602	2.325	4.905	7.396	2.419
T_{Dominant} **(s)**	0.868	0.489	0.492	0.898	0.408	0.401
Records on Soil						
Earthquake	**Bam**	**Loma Prieta**	**Kobe**	**Northridge**	**Mammoth Lakes**	**Imperial Valley**
Date	**26/12/2003**	**18/10/1989**	**16/1/1995**	**17/1/1994**	**25/5/1980**	**15/10/1979**
Station	**Bam**	**Gilroy#2**	**Takatori**	**Sylmar**	**54099 Convict Creek**	**5028 El Centro Array #7**
Component	**L**	**000**	**000**	**360**	**180**	**140**
PGA **(m/s/s)**	7.783	3.603	5.998	8.273	4.33602	3.31578
PGV **(m/s)**	1.235	0.329	1.271	1.296	0.231	0.476
PGD **(m)**	0.343	0.072	0.358	0.327	0.054	0.247
Soil Type (Geomatrix)	Soil	Deep (broad) soil	Soft (deep) soil	Deep (broad) soil	Deep (broad) soil	Deep (broad) soil
$T_{(\text{total})}$ **(s)**	66.560	39.950	40.960	40.000	29.955	36.820
$T_{(\text{Page-Bolt})}$ **(s)**	39.225	12.760	31.750	12.740	14.350	8.035
T_{Trifunac} **(s)**	8.004	10.978	11.343	5.317	9.345	6.825
CAV **(m/s)**	22.225	8.170	26.000	14.156	12.116	6.394
a_{rms} **(m/s/s)**	1.125	0.765	1.308	1.568	1.067	0.817
I_a **(m/s)**	7.946	1.197	8.697	5.012	2.619	0.858
I_c **(m$^{1.5}$/S$^{2.5}$)**	7.471	2.392	8.428	7.005	4.179	2.093
C.F. **(Hz)**	6.175	3.391	2.128	3.022	8.360	2.889
S.F.	0.604	0.581	0.720	0.623	0.529	0.739
M.P.A. **(m/s/s)**	4.061	2.325	4.228	4.768	3.642	2.360
T_{Dominant} **(s)**	0.997	0.756	1.331	0.984	0.335	0.902

Table 2. Damage states based on Park & Ang damage index.

Damage State		*DT*	
		Range	Best Estimate
1	Nonstructural damage	0.01-0.10	0.05
2	Slight structural damage	0.10-0.20	0.15
3	Moderate structural damage	0.20 - 0.50	0.35
4	Severe structural damage	0.50 - 0.85	0.67
5	Collapse	0.85 - 1.15	1.00

where:

$DT_i =$ Damage index corresponding to the ith damage state,
$F_{DT}(.) =$ Probability distribution function of DT.

Considering log-normal distribution for DT, PF_{ij} would be calculated as follows:

$$PF_{ij} = 1 - \Phi\left(\frac{\ln(DI_i) - \overline{\ln(DI)}}{\sigma_{\ln(DI)}}\middle| CAV = v_j\right), \quad (4)$$

where:

$\Phi() =$ Normal distribution function,
$\overline{\ln(DI)} =$ Mean natural logarithm of damage index,
$\sigma_{\ln(DI)} =$ Standard deviation of logarithm of damage index.

The fragility curve, with respect to the ith damage state, can be constructed using PF_{ij} values at various CAV levels.

The damage probability matrix shows the probability that the damage occurred will be located in a specific damage state. The probability PDS_{ij}, which shows that the damage to a structure caused by an earthquake with CAV equal to v_j is in the ith damage state, can be derived from the fragility data as follows:

$$PDS_{ij} = \begin{cases} PF_{ij} - PF_{i+1j} & (i \leq 4) \\ PF_{ij} & (i = 5) \end{cases} \quad (5)$$

The damage index can be related to earthquake loss through using a damage cost function. In this way, the Annual Earthquake Loss (AEL) of a structure is determined.

PROPERTIES OF THE MATERIALS

Several laboratory experiments have been done on the behavior of masonry in various regions around the world [12]. To consider uncertainty in structural parameters, first, a probabilistic distribution is assigned to each of them [10]. Then, by using the Monte Carlo Simulation method [8], 15 different values have been generated for each structural parameter, based on its distribution function. These parameters, with their assigned average value, type of distribution function and coefficient of variation, are shown in Table 3. The average compressive and tensile strength of traditional brick laying in Iran are considered to be 5 and 0.6 MPa, respectively [13].

NUMERICAL MODELING OF THE BUILDINGS

The nonlinear analysis program, IDARC 4.0 [9], is used to model the buildings and calculate the damage indices. Reinforced concrete buildings, steel buildings and masonry infill panels can be modeled using this program. But, the models for masonry buildings cannot be generated directly using IDARC. By comparing brick and concrete, it can be recognized that both have similar properties. Although there is a long gap between their compressive strength, they both behave much stronger in compression, so, their tensile strength is almost abandoned. Consequently, in this paper, an unreinforced masonry panel is modeled as a concrete shear wall without any reinforcement. The assumed stress-strain curves for masonry and concrete in IDARC are shown in Figure 2.

The behavior of brick can be simulated by using a concrete stress-strain model, through considering equivalent values for corresponding parameters in their stress-strain diagrams. These parameters include: Compressive and tensile strength, strain corresponding to compressive strength, ultimate strain and the slopes of the initial and descending sections of the diagram (Figure 2).

The structural elements used to model masonry buildings in this research include beams, shear walls and edge columns, as presented in Figure 3, with their assigned degrees of freedom.

Table 3. Material properties with their average value, type of distribution function and coefficient of variation.

Parameter	Average Value (Mpa)	Distribution Function Type	COV
Compressive Strength of Brick Laying	5	Normal	0.13
Tensile Strenath of Brick Lavina	0.6	Normal	0.17
Compressive Strenath of Concrete	21	Normal	0.17
Tensile Strength of Reinforcing Bars	220	Log-Normal	0.07

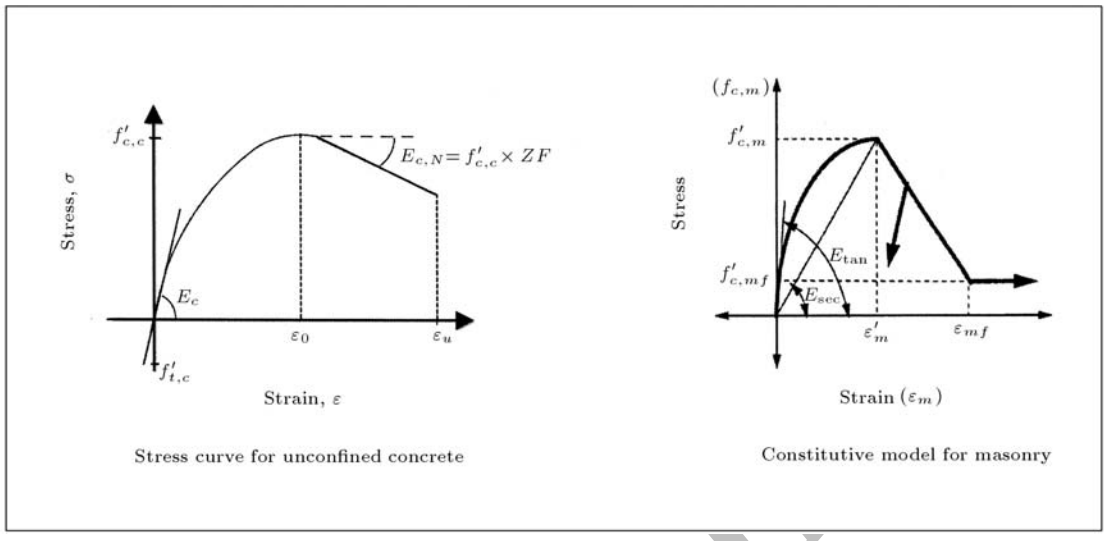

Figure 2. Stress-strain curve for masonry and concrete in IDARC program.

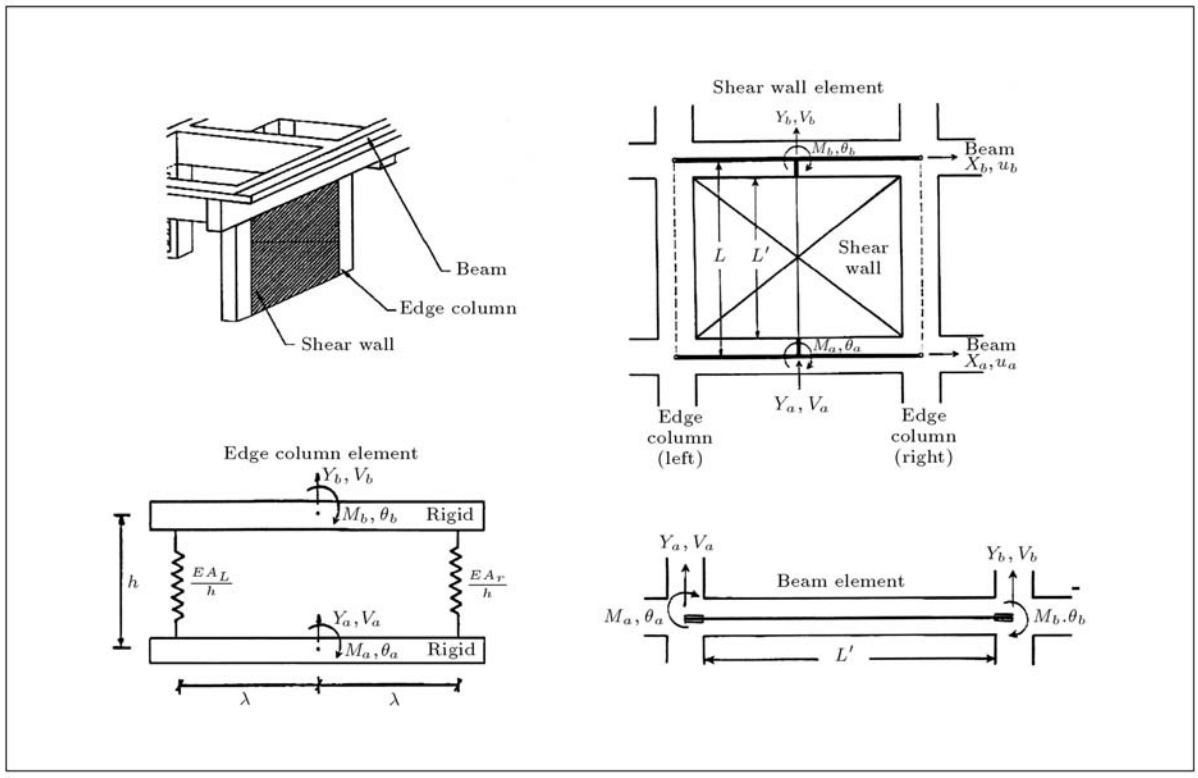

Figure 3. Structural elements used in modeling masonry buildings (IDARC 4.0 [9]).

As stated earlier, in this paper, masonry walls have been modeled as shear wall elements, substituting concrete properties with those of masonry. Verticals ties are modeled as edge columns, since they behave as axial members, keeping the integrity of the building in a vertical direction, and horizontal ties are modeled as beam elements.

Flexural, shear and axial deformations are considered in the modeling of shear wall elements in IDARC 4.0 [9]. Flexural and shear deformations are modeled using one of the four different hysteretic models:

a) Three parameter Park model,

b) Three parameter steel model,

c) Bilinear model,

d) Linear-elastic model.

These different hysteretic models, with their corresponding parameters, are discussed fully in the IDARC manual. The axial deformation component is modeled as a linear-elastic spring and the cracking and shear strengths, V_c and V_y, are determined from the following empirical relations:

$$V_c = \frac{0.6(f'_c + 7.11)}{M/(VL_w) + 1.7} b_e L_w, \tag{6}$$

$$V_y = \left\{ \frac{0.08\rho_t^{0.23}(f'_c + 2.56)}{M/(VL_w) + 0.12} + 0.32\sqrt{f_y \rho_w} + 0.1 f_a \right\} b_e L_w, \tag{7}$$

where $M(VL_w)$ is the shear span ratio; ρ_t is the tension steel ratio in percent; ρ_w is the wall reinforcement ratio; f_a is the axial stress; b_e is the equivalent web thickness and L_w is the distance between the edge columns.

Five different types of building are modeled in this study: One and three-story URM (Un-Reinforced Masonry), with and without ties, and a one-story reinforced masonry building. To obtain fragility curves for each type of building, 450 nonlinear analyses are performed, based on various models, earthquake records and the CAV values used in generating these curves.

Each building is considered 5 m $\times$ 5 m in plan and each story is 3 m high. The thickness of the masonry walls is assumed to be 0.3 m. The plan and elevation of these buildings are shown in Figure 4. If horizontal or vertical ties are provided, they are used, according to the Iranian Seismic Code [14]. Each tie is 0.3 $\times$ 0.3 m in section, including four ϕ12 reinforcing bars and ϕ6 stirrups with 0.2 m spacing. For retrofitting the masonry walls, reinforcing bars are distributed horizontally and vertically in the walls in addition to ties. After designing the masonry walls to resist seismic loading, the required percentage of horizontal and vertical reinforcement in each wall was turned into 0.3%. To satisfy these requirements of reinforcement, 24ϕ12 are used horizontally and 40ϕ12 vertically in each wall.

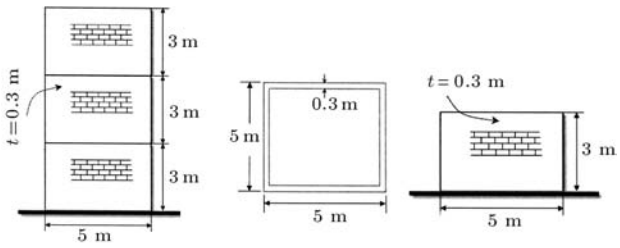

Figure 4. Plan and elevations of masonry buildings considered in study.

NONLINEAR ANALYSIS RESULTS AND CORRESPONDING FRAGILITY CURVES

In Figure 5, fragility curves and corresponding damage matrices are presented for each type of masonry building mentioned before. These diagrams are obtained separately on hard rock and soil sites, in order to determine the effects of soil type on the seismic behavior of these buildings.

EARTHQUAKE LOSS

In this paper, the cost of damage to a building resulted from an earthquake is considered to be the direct cost of repairing that building and does not include the cost due to loss of building functions after the earthquake. CDR_i, the central damage cost ratio, is defined as the ratio of the mean repair cost of a building in the ith damage state to the replacement cost of that building [10].

In this paper, CDR values, proposed in FEMA 1985, are used to estimate earthquake loss to different types of masonry building, as previously discussed (Table 4).

The damage cost ration, $\overline{DR}_j$, due to an earthquake with $CAV = v_j$ can be calculated as follows:

$$\overline{DR}_j = \sum_{i=1}^{5} PDS_{ij} \times CDR_i. \tag{8}$$

Then, the damage cost, DC_j, given the occurrence of an earthquake with $CAV = v_j$, would be determined as follows:

$$DC_j = \overline{DR}_j \times (\text{replacement cost of building}). \tag{9}$$

Assuming the occurrence of an earthquake, the expected annual earthquake loss, AEL, of the building is calculated as follows:

$$AEL = \sum_{j=1}^{N_a} DC_j . \left\{ F_v\left(v_j + \frac{\Delta v}{2}\right) - F_v\left(v_j - \frac{\Delta v}{2}\right) \right\}, \tag{10}$$

Table 4. Damage cost ratios corresponding to various damage states (FEMA 1985).

	Damage State	Damage Cost Ratio Range (%)	Central Damage Cost Ratio (%)
0	No damage	0 - 0.05	0
1	Minor nonstructural	0.05 - 1.25	0.3
2	Slight	1.25 -7.5	3.5
3	Moderate	7.5 - 20	10
4	Severe	20 - 90	65
5	Collapse	90 - 100	95

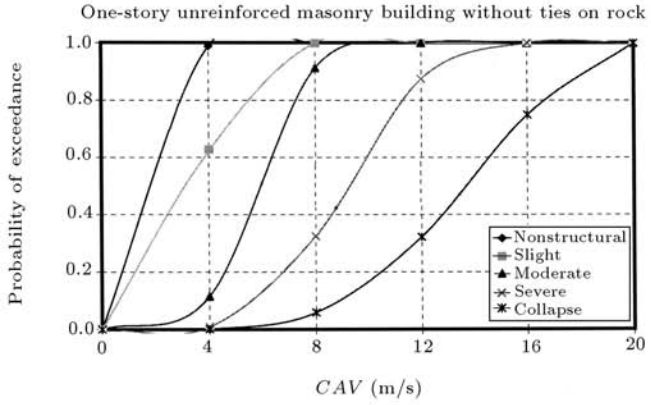

CAV (m/s)	Non-Structural	Slight	Moderate	Severe	Collapse
4	0.365	0.510	0.106	0.008	0.001
8	0.000	0.088	0.587	0.266	0.059
12	0.000	0.000	0.127	0.551	0.322
16	0.000	0.000	0.000	0.251	0.749
20	0.000	0.000	0.000	0.000	1.000

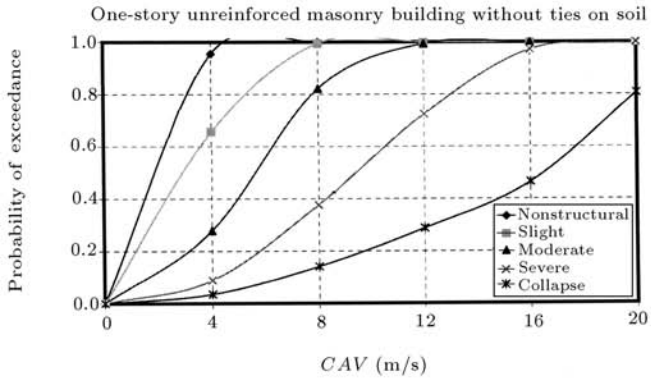

CAV (m/s)	Non-Structural	Slight	Moderate	Severe	Collapse
4	0.298	0.379	0.189	0.054	0.034
8	0.006	0.173	0.445	0.236	0.141
12	0.000	0.007	0.269	0.438	0.287
16	0.000	0.000	0.029	0.506	0.465
20	0.000	0.000	0.000	0.194	0.806

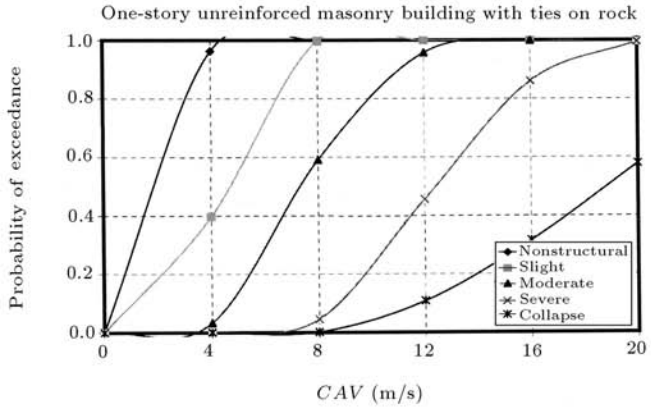

CAV (m/s)	Non-Structural	Slight	Moderate	Severe	Collapse
4	0.565	0.364	0.032	0.001	0.000
8	0.003	0.405	0.547	0.043	0.002
12	0.000	0.042	0.502	0.349	0.107
16	0.000	0.000	0.139	0.545	0.316
20	0.000	0.000	0.004	0.417	0.579

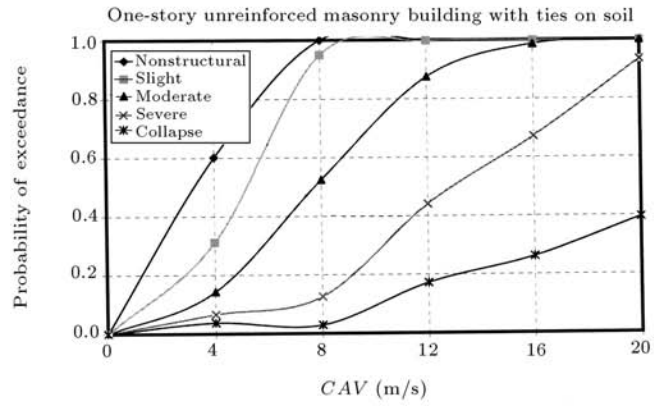

CAV (m/s)	Non-Structural	Slight	Moderate	Severe	Collapse
4	0.290	0.169	0.077	0.028	0.037
8	0.050	0.425	0.400	0.096	0.029
12	0.002	0.123	0.433	0.269	0.172
16	0.000	0.014	0.314	0.410	0.262
20	0.000	0.000	0.067	0.538	0.395

Figure 5. Fragility curves and corresponding damage probability matrices for each type of masonry building on hard rock and soil.

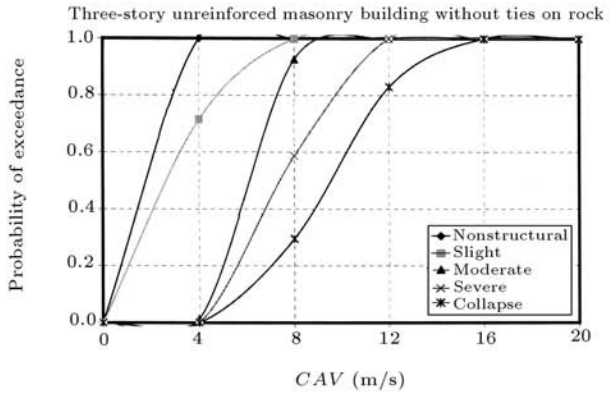

CAV (m/s)	Non-Structural	Slight	Moderate	Severe	Collapse
4	0.285	0.701	0.013	0.000	0.000
8	0.001	0.072	0.339	0.292	0.295
12	0.000	0.000	0.000	0.171	0.829
16	0.000	0.000	0.000	0.000	1.000
20	0.000	0.000	0.000	0.000	1.000

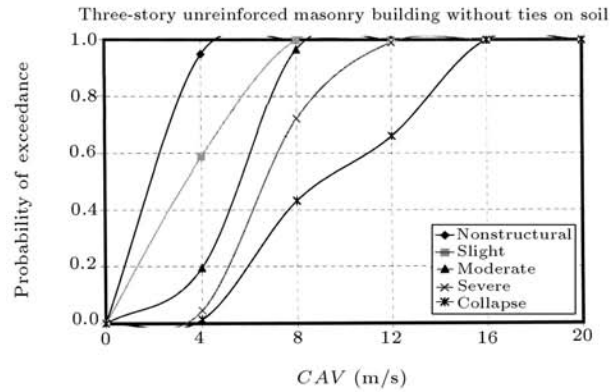

CAV (m/s)	Non-Structural	Slight	Moderate	Severe	Collapse
4	0.360	0.394	0.149	0.032	0.014
8	0.000	0.034	0.244	0.290	0.432
12	0.000	0.000	0.010	0.330	0.660
16	0.000	0.000	0.000	0.000	1.000
20	0.000	0.000	0.000	0.000	1.000

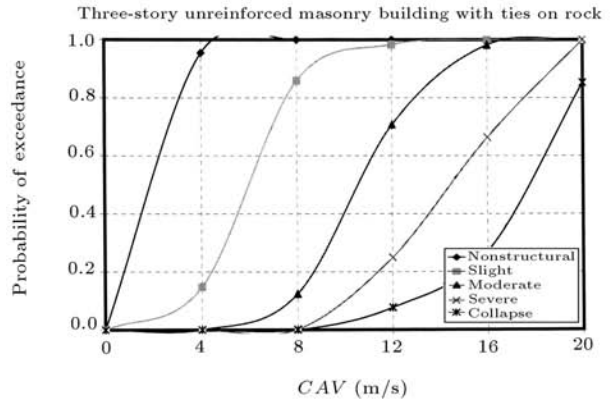

CAV (m/s)	Non-Structural	Slight	Moderate	Severe	Collapse
4	0.806	0.147	0.001	0.000	0.000
8	0.142	0.734	0.122	0.002	0.000
12	0.016	0.276	0.458	0.173	0.077
16	0.000	0.018	0.319	0.393	0.270
20	0.000	0.000	0.000	0.148	0.852

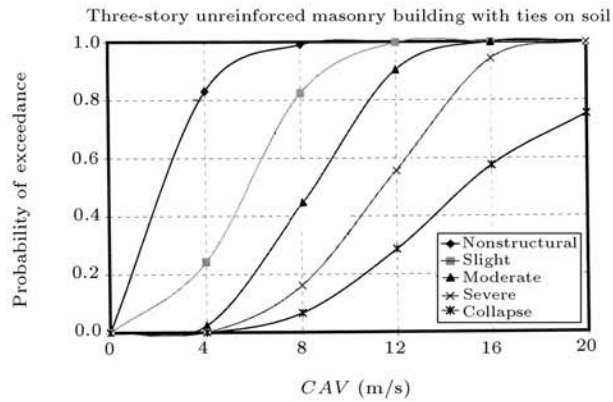

CAV (m/s)	Non-Structural	Slight	Moderate	Severe	Collapse
4	0.587	0.219	0.023	0.001	0.000
8	0.166	0.386	0.277	0.095	0.067
12	0.002	0.094	0.345	0.273	0.286
16	0.000	0.000	0.057	0.367	0.576
20	0.000	0.000	0.000	0.246	0.753

Figure 5. Fragility curves and corresponding damage probability matrices for each type of masonry building on hard rock and soil (continued).

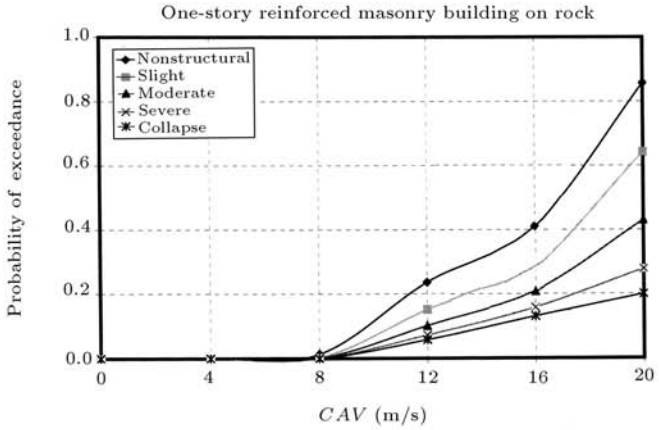

CAV (m/s)	Non-Structural	Slight	Moderate	Severe	Collapse
4	0.000	0.000	0.000	0.000	0.000
8	0.014	0.004	0.001	0.000	0.000
12	0.122	0.065	0.034	0.015	0.040
16	0.147	0.104	0.069	0.037	0.174
20	0.151	0.116	0.082	0.046	0.239

Figure 5. Fragility curves and corresponding damage probability matrices for each type of masonry building on hard rock and soil (continued).

where, $F_v()$ is the probability distribution function of CAV in one year.

The calculated values of the mean damage cost ratio for the five types of masonry building considered in this research are presented in Table 5, corresponding to different values of CAV. As seen in this table, by providing vertical and horizontal ties and by reinforcing masonry buildings, earthquake loss significantly reduces.

COMPARISON AND SENSITIVITY ANALYSIS OF THE FRAGILITY CURVES

In this section, fragility curves and mean damage indices are compared, in order to show the influence of some parameters on the seismic behavior of masonry buildings. These parameters include: Number of stories, soil type, vertical and horizontal ties and reinforcing bars.

In Figure 6, it is observed that the structural damage increases with an increase in the number of stories, from one to three, and the difference becomes more significant in severe states of damage.

As seen in Figure 7, for low values of CAV, the nonlinear effect of the soil becomes dominant and increases damage indices. But, as CAV increases, the structural damage on the rock becomes predominant. This seems to be consistent, because of the fact that the dominant period of rocky ground is more comparable to the natural period of a one-story masonry building than that of ground made of soil. Totally, however, there is no significant difference between the fragility curves and damage indices of one-story masonry buildings on rock and soil, since the

Table 5. Calculated values of mean damage cost ratio for masonry buildings considered in this study.

Mean Damage Cost Ratio (%) for Masonry Buildings Located on Rock					
CAV (m/s)	**1S-UR-W/O[a]**	**1S-UR-W[b]**	**3S-UR-W/O[c]**	**3S-UR-W[d]**	**1S-R[e]**
4	3.6	1.8	2.7	0.8	0.0
8	29.1	9.9	50.6	4.0	0.0
12	67.7	38.0	89.9	24.1	6.9
16	87.5	66.8	95.0	54.4	15.0
20	95.0	82.2	95.0	90.6	26.5
Mean Damage Cost Ratio (%) for Masonry Buildings Located on Soil					
CAV (m/s)	**1S-UR-W/O**	**1S-UR-W**	**3S-UR-W/O**	**3S-UR-W**	**1S-R**
4	10.0	6.8	6.4	1.2	0.0
8	33.8	14.5	62.4	16.7	0.0
12	58.4	38.6	84.3	48.7	5.4
16	77.4	54.7	95.0	79.1	20.0
20	89.2	73.2	95.0	87.5	27.0

(a): 1Story UnReinforced WithOut; (b): 1Story UnReinforced With ties; (c): 3Story UnReinforced WithOut ties; (d): 3Story UnReinforced With ties; (e): 1Story Reinforced.

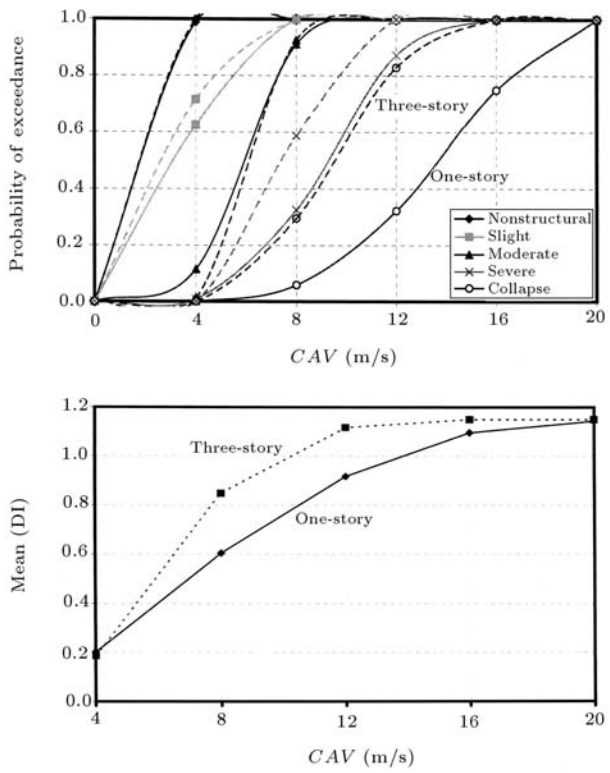

Figure 6. The effect of number of stories on fragility curves and mean damage index values in unreinforced masonry buildings without ties on rock.

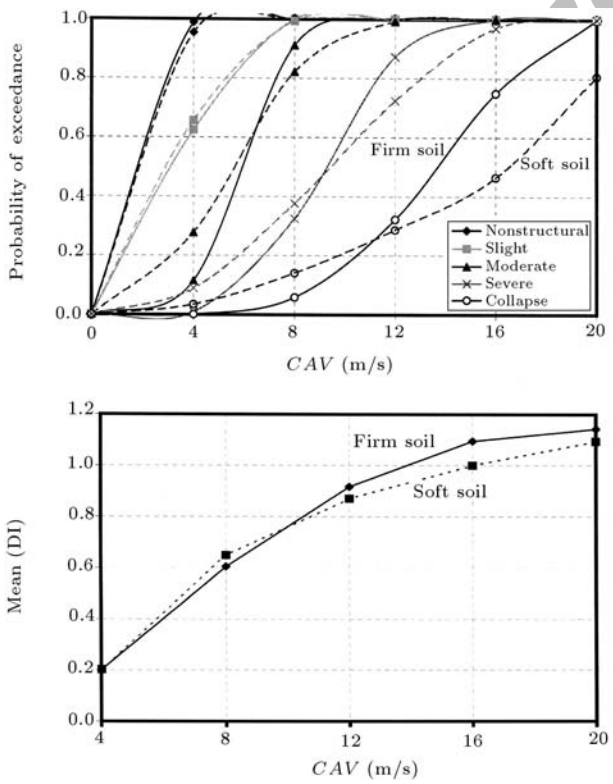

Figure 7. The effect soil type on fragility curves and mean damage index values in one-story unreinforced masonry building without ties.

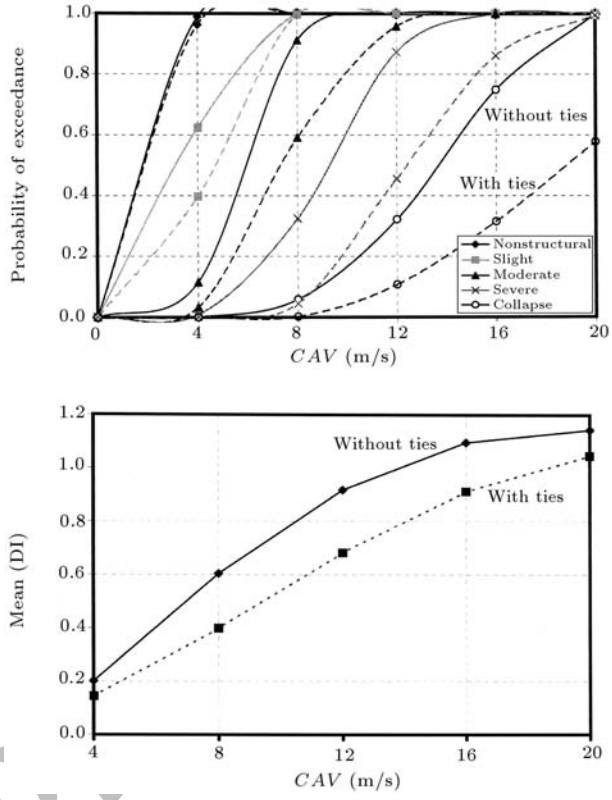

Figure 8. The effect of using ties on fragility curves and mean damage index values in one-story unreinforced masonry buildings on rock.

nonlinear effect of soil would not greatly influence short buildings.

In Figure 8, the significant difference between fragility curves in severe states of damage for one-story masonry buildings, before and after using ties, shows the effectiveness of horizontal and vertical ties, in reducing structural damage in masonry buildings. It is seen that the difference almost increases with CAV.

As shown in Figure 9, retrofitting masonry walls with horizontal and vertical reinforcements substantially decreases the structural damage to masonry buildings. This influence is so significant that even the fragility curve for the nonstructural state of damage after retrofitting is far below the one for the collapse state of damage before retrofitting.

A CORRESPONDENCE BETWEEN FRAGILITY CURVES AND PUSHOVER DIAGRAM

The pushover diagram of a structure is the result of a nonlinear static analysis under an increasingly monotonic force. Any point on the pushover diagram of a structure can be related to the corresponding point on the fragility curves of that structure, as shown in Figure 10.

Through using the following equations, F, is the

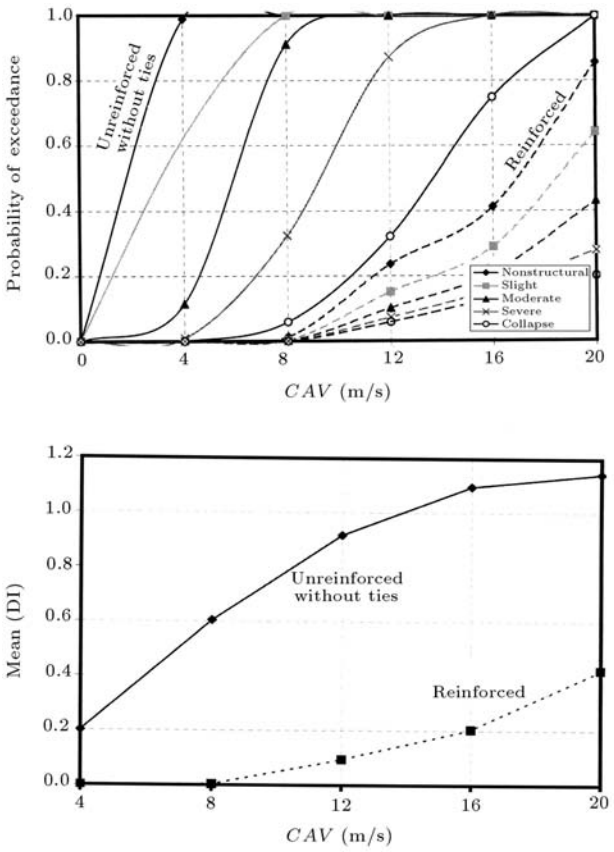

Figure 9. The effect of reinforcement on fragility curves and mean damage index values in one-story masonry buildings on rock.

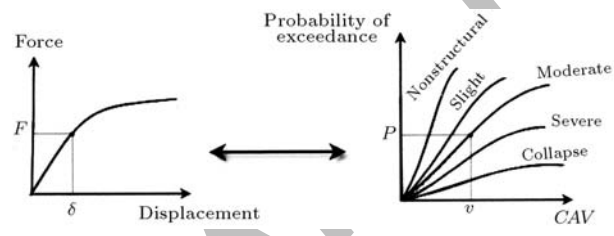

Figure 10. A correspondence between fragility curves and pushover diagram of a structure.

base shear, which is related to peak ground acceleration as follows [14]:

$$F = \frac{ABI}{R}W, \tag{11}$$

where:

A	=	Peak ground acceleration (g),
B	=	Structure response coefficient,
I	=	Importance factor,
R	=	Structure behavior factor,
W	=	Structure weight,

For masonry buildings, $R = 4$, $I = 1$ and $B = 2.5$ (period < 0.4 s). Hence, Equation 9 becomes:

$$F = \frac{A \times 2.5 \times 1.0}{4}W \Rightarrow A = 1.6\frac{F}{W}. \tag{12}$$

Then, CAV can be estimated, based on the resulted peak ground acceleration using Figure 1. The obtained value for CAV corresponds to the different probabilities of exceedance in each state of damage on the fragility curves (point (p, v)) in Figure 10.

The damage index can be evaluated from the pushover diagram of a structure, using each of the following equations [11]:

$$DI_\mu = \frac{\delta_m - \delta_y}{\delta_u - \delta_y}, \tag{13}$$

$$FDR = \frac{k_0}{k_f} \times \frac{k_m - k_0}{k_f - k_0}, \tag{14}$$

where:

δ_m	=	Maximum displacement due to an increasingly monotonic load,
δ_y	=	Yield displacement,
δ_u	=	Failure displacement months after the publication date of the paper.

k_0, k_m, k_f are initial, maximum and failure stiffness, respectively, as defined in Figure 11.

The state of damage to the structure is determined, based on the obtained damage index from the pushover diagram. The probability of exceeding this damage state, corresponding to the value of CAV previously obtained, can be estimated from the fragility curves of the structure and it should result in a reasonable value, since this state of damage has actually occurred.

COMPARISON WITH OTHER STUDIES

A comparison is done between the fragility curves obtained in this study and the resulted fragility curves

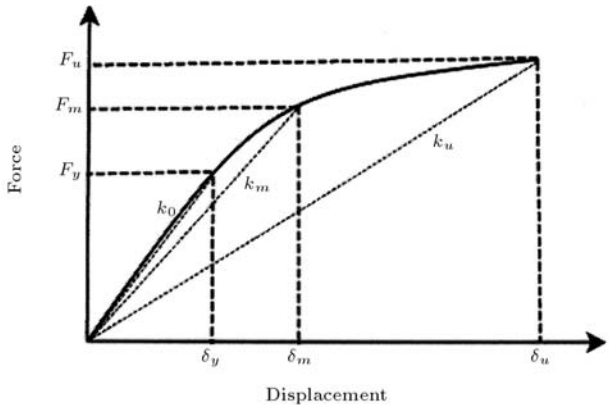

Figure 11. Definition of δ_y, δ_m, δ_u, k_0, k_m, k_u on the pushover diagram.

for 1-story unreinforced masonry buildings in Memphis city, under simulated ground motion, in a report by Abrams and Shinozuka, although the method of developing the fragility curves in this study is completely different from the one used in their studies [6]. The dimensions of the 1-story masonry building presented in their study are shown in Figure 12.

In Figure 13, the corresponding fragility curves for this building are shown, in comparison with the ones obtained in this research, for 1-story unreinforced masonry buildings located on hard rock. It should be noticed that these buildings are different, according to dimensions, openings, soil type and some other parameters. Also, the seismic intensity parameter differs in the two diagrams and a general comparison would be appropriate. As seen in Figure 13, for moderate earthquakes, with $CAV = 8$ m/s (or, equivalently, $PGA = 0.4$ g (refer to Figure 1)), the probability of a slight damage state occurring (equivalent to cracking in the fragility curves by Abrams and Shinozuka) for these type of buildings is 100%, as in Figure 13a and 90%, as in Figure 13b. This probability becomes 30% for a severe damage state, as in Figure 13a. and 20%, as in Figure 13b, while the probability of collapse is negligible in both diagrams.

CONCLUSIONS

Fragility curves provide a powerful tool for anticipating the damage to structures in future probable earthquakes. Also, the effect of different parameters on the seismic behavior of these structures can be investigated through using fragility curves.

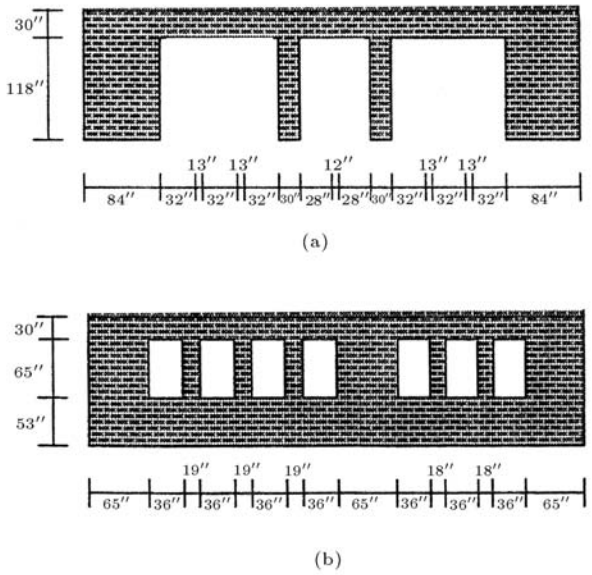

Figure 12. Elevations of the 1-story unreinforced masonry building in the study by Abrams and Shinozuka [6]; (a) Door wall; (b) Window wall.

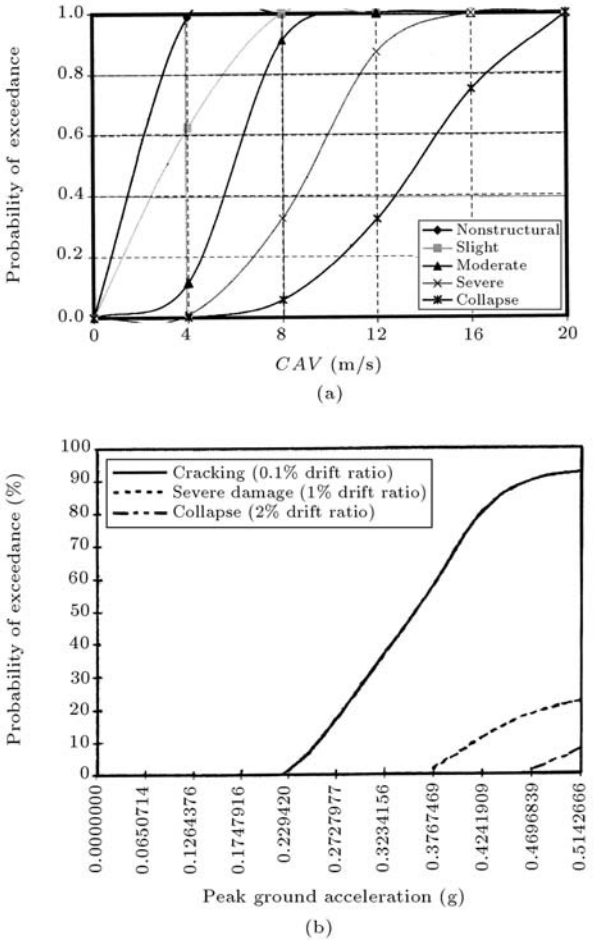

Figure 13. Comparison of fragility curves obtained (a) in this study and (b) by Abrams and Shinozuka [6], for 1-story unreinforced masonry building without ties.

For the most probable earthquakes, which are the ones with moderate intensity (0.2 g $< PGA <$ 0.5 g, equivalent to 5 m/s $< CAV <$ 12 m/s, (refer to Figure 1)), following results could be recognized:

1. In one-story unreinforced masonry buildings without ties, nonstructural and slight damage definitely occur and moderate damage is, therefore, probable. The probability of occurring severe damage is, approximately, 35% and the probability of collapse is less than 20%;
2. In one-story unreinforced masonry buildings with ties, nonstructural and slight damage will certainly occur. The probability of occurring moderate damage is almost 60% and the probability of more severe damage and collapse is insignificant;
3. In three-story unreinforced masonry buildings without ties, nonstructural, slight and moderate damage states are completely possible. The probability of occurring severe damage is more than 60% and the probability of collapse is between 30% and 45%;
4. In three-story unreinforced masonry buildings with

ties, nonstructural and slight damage states are very probable. The probability of occurring moderate damage is between 10% and 45% and the probability of severe damage and collapse is negligible;

5. In one-story reinforced masonry buildings, the probability of each state of damage occurring is negligible.

In addition, soil type does not have a significant effect on the fragility curves of masonry buildings, especially in less destructive states of damage and especially for short buildings (one-story).

The obtained results in this study verify that the minimum requirements incorporated in the seismic provisions of modern codes, in order to improve the performance of URM buildings in earthquakes, are really effective.

Based on the relation found between fragility curves and the pushover diagram of a structure, analytical fragility curves can be updated, using the pushover diagram of the structure, which is resulted from either a nonlinear static analysis or an experiment.

REFERENCES

1. Bakhshi, A., Tavallali, H. and Karimi, K. "Evaluation of structural damage using simplified methods", *Journal of European Earthquake Engineering*, **3**, pp 61-68 (2007)
2. Shinozuka, M. et al. "Statistical analysis of fragility curves", *Journal of Engineering Mechanics*, **126**(12), pp 1224-1231 (2001).
3. Mackie, K. and Stojadinovic, B. "Fragility curves for reinforced concrete highway overpass bridges", *Proceedings of the 13th World Conference on Earthquake Engineering*, Vancouver, B.C., Canada (2004).
4. Dumova-Jovanoska, E. "Fragility curves for reinforced concrete structures in Skopje (Macedonia) region", *Journal of Soil Dynamics and Earthquake Engineering*, **19**, pp 455-466 (2000).
5. Singhal, A. and Kiremidjian, A.S. "A method for earthquake motion-damage relationship with application to reinforced concrete frames", *Technical Report NCEER-97-0008*, State University of New York at Buffalo, USA (1997).
6. Abrams, D.P. and Shinozuka, M. "Loss assessment of Memphis buildings", *Technical Report NCEER-97-0018*, State University of New York at Buffalo, USA (1997).
7. Tantala, M.W. and Deodatis, G. "Development of seismic fragility curves for tall buildings", *Proceedings of the 15th ASCE Engineering Mechanics Conference*, New York, USA (2002).
8. Rubinstein, R.Y., *Simulation and The Monte Carlo Method*, John Wiley & Sons, New York, NY (1989).
9. Reinhorn, A., Valles, R.E. et al. "IDARC 2D version 4, a program for inelastic damage analysis of RC structures", State University of New York at Buffalo, USA (1995).
10. Hwang, H.H.M. and Huo, J-R. "State generation of hazard-consistent fragility curves for seismic loss estimation studies", *Technical Report NCEER- 94-0015*, State University of New York at Buffalo, USA (1994).
11. Williams, M.S. and Sexsmith, R.G. "Seismic damage indices for concrete structures: A state-of-the-art review", *Earthquake Spectra*, **11**(2), pp 319-349 (1995).
12. Mayes, R.L. and Clough, R.W. "State of the art in seismic shear strength of masonry: an evaluation and review", *Report EERC 75-21*, University of California, Berkeley, California, USA (1975).
13. Moghaddam, H., *Seismic Design of Masonry Buildings*, Sharif University of Technology Publications, Tehran, I.R. Iran (1994).
14. Building & Housing Research Center, *Iranian Code of Practice for Seismic Resistant Design of Buildings*, Standard No. 2800, 2nd Ed. (1999).